Numerical Simulation of Upwelling Flow in Pipe Generated by Perpetual Salt Fountain

Tetsuya SATO[1], Shigenao MARUYAMA[2], Atsuki KOMIYA[2] and Koutaro TSUBAKI[3]

[1]Graduate School of Engineering
Tohoku University, Sendai, Miyagi, 980-8579 JAPAN
[2]Institute of Fluid Science
Tohoku University, Sendai, Miyagi, 980-8577 JAPAN
[3]Department of Mechanical Engineering
Saga University, Saga, Saga, 840-8502 JAPAN

Abstract

Upwelling of deep seawater to the region, where sunlight reaches, can produce the ocean farm since deep seawater contains high concentration of nutrient. The numerical simulation for upwelling of deep seawater with the perpetual salt fountain proposed by Stommel et al. was conducted in this study. The temperature and salinity distributions measured in Mariana area where the upwelling experiment was conducted by Maruyama et al. was used. As a result, the velocity profile of the upwelling experiment was predicted as M-shape flow and the flow rate was estimated as 43t/day in the pipe. Additionally the possibility of reverse flow in the pipe was indicated. Furthermore the possibility of upwelling in other ocean areas using the results was discussed. As a result, it became clear that the unified representation of ocean conditions was achieved by the new dimensionless number Ra_R, which was modified Rayleigh number, and flow rate in the pipe could be evaluated by Ra_R.

Introduction

The great increase of the world population has required greater food productivity. However, an expansion of farm production has been limited by the deforestation problem. In contrast, pelagic zone has large areas but has low biological productivity. These are classified as ocean desert. The fertilization of pelagic zone may solve a problem with food product.

One of the methods for the fertilization of ocean desert is an effective utilization of deep seawater. Deep seawater, which is deeper than 200m, has rich nutrient concentration as compared to epipelagic seawater [6]. Therefore if it is possible to draw up deep seawater to photic zone, the sea cultivation can be created in ocean desert.

Generally a pump has been used for upwelling of deep seawater. For example, the upwelling experiment has been conducted in Sagami bay, Japan [7]. However a pump requires a large amount of energy and a periodic maintenance. Furthermore the drawn up water may sink because it is drawn up with keeping low temperature. Therefore a pump is not suitable system for the artificial upwelling in pelagic zone.

Maruyama et al. proposed the upwelling of deep seawater in pelagic zone using the perpetual salt fountain proposed by Stommel et al. [1,5]. In many tropical and subtropical regions, salinity and temperature of epipelagic seawater are higher than those of deep seawater. When a pipe is settled in such stratification and then filled with low salinity deep seawater, the inside temperature distribution along the pipe axis becomes same as outside one eventually. As a result, buoyancy force occurs in the pipe because inside salinity is lower than outside one. The
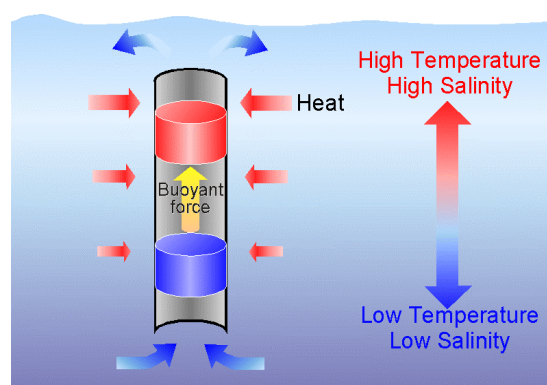

Figure 1. Concept of the perpetual salt fountain

concept of the perpetual salt fountain is shown in Figure 1. This buoyancy force induces the upwelling flow in the pipe and it continues as long as temperature and salinity difference between epipelagic and deep seawater exist. The artificial upwelling does not need external energy except the initial input.

Tsubaki et al. conducted upwelling experiment in 2002 using the perpetual salt fountain in Mariana area, which lies in 142.24E and 11.25N of pelagic zone. A tracer was ejected in the pipe and one tracer sensor was laid 2m downstream of ejector to observe the upwelling flow. The upwelling velocity and tracer diffusivity was measured for the first time in the world [5]. However measured diffusivity was 10^4 times as large as molecular diffusivity. They predicted that this was the effect of many vortices produced by deformed and oscillated pipe.

Zhang et al. conducted numerical simulation related to ocean experiment to predict flow field in the pipe [8]. The measured diffusivity was specified as eddy diffusivity in that calculation. As a result, agreement between numerical and experimental results was observed and velocity profile in the pipe was estimated as M-shape flow. However they compared the numerical result with the experimental one at only one point because one sensor was installed in the experiment. Therefore numerical result of velocity profile was partially reliable.

Accordingly in this paper, the numerical simulation was conducted again and the results were compared with experimental one at two sensor points, which were laid 2m and 5m downstream of the ejection. Then exact flow rate estimation at Mariana area was discussed. These sensor data were obtained after foregoing calculation [2]. Furthermore, as a first step for estimation of sea cultivation in other ocean area, the possibility of flow rate estimation in other ocean area was studied.

Numerical Simulation

Figure 2 is the calculation domain considered in this study. This domain shows a portion of ocean including the pipe and the top boundary represents ocean surface. The left boundary is specified as the pipe axis and the top and bottom boundary are specified as adiabatic wall. The right boundary is specified as the wall, which has ocean temperature. The pipe length and location correspond to ocean experiment. This domain is set large enough to take no notice of wall effect.
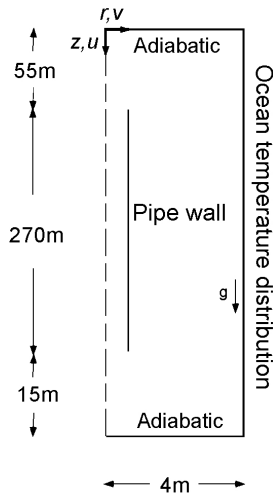

Figure 2. Calculation domain and coordinate system

The governing equations are as follows.

$$\nabla \cdot (\rho \mathbf{V}) = 0 , \tag{1}$$

$$\frac{\partial(\rho \mathbf{V})}{\partial t} + \nabla \cdot (\rho \mathbf{VV}) = \nu \nabla^2 \mathbf{V} - \nabla P + \rho \mathbf{g} , \tag{2}$$

$$\frac{\partial(\rho T)}{\partial t} + \nabla \cdot (\rho \mathbf{V}T) = \frac{k}{c_p} \nabla^2 T , \tag{3}$$

$$\frac{\partial(\rho C)}{\partial t} + \nabla \cdot (\rho C\mathbf{V}) = \nabla \cdot (\rho D \nabla C) , \tag{4}$$

where ρ, ν, k, c_p are density, kinematic viscosity, thermal conductivity and specific heat, respectively. The vectors $\mathbf{V}$, $\mathbf{g}$ are velocity and gravity, T, C, D are temperature, concentration and mass diffusivity, respectively.

The fluid outside the pipe is specified as steady temperature and salinity distributions, which were measured in ocean experiment in 2002, as shown in Figure 3 [5]. The fluid inside the pipe is specified as constant salinity, which was measured at the bottom of the pipe. At initial time, temperature distribution inside the pipe is specified as that outside the pipe.

In this study, the measured diffusivity $10^{-5} \text{m}^2/\text{s}$ is assumed to be eddy diffusivity. Therefore eddy diffusivity becomes much larger than molecular diffusivity. As a result, eddy thermal diffusivity and eddy kinetic viscosity can be assumed to be same as eddy diffusivity. In this study, the mass diffusivity, D, in eq. (4) is specified as the eddy diffusivity. Furthermore the thermal diffusivity and kinematic viscosity are also specified as the eddy diffusivity. Thermal conductivity and viscosity, which are calculated with eddy diffusivity, are used in eqs. (2) and (3). The density is calculated by UNESCO's equation, which assumes density as a function of temperature, salinity and pressure [4]. Other properties are assumed to be constant.
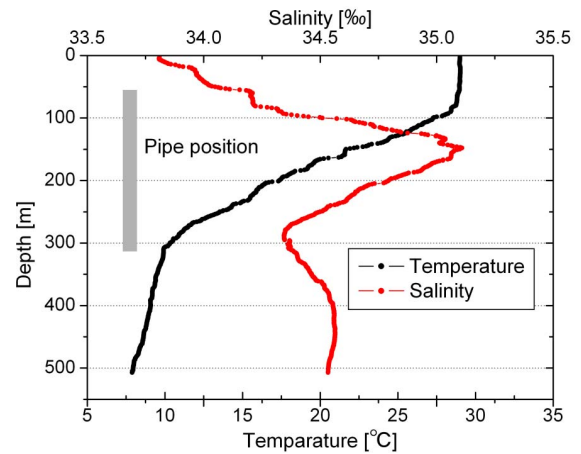

Figure 3. Temperature and salinity distributions in Mariana area

The numerical simulation code is built with FLUENT 6.3.13, a commercial CFD package. An unsteady simulation is conducted with first order implicit method. A structured non-uniform grid is used. The convection terms are modelled with second-order upwind scheme and the diffusion terms are modelled with second-order central scheme. The SIMPLE algorithm is used for pressure correction.

There are two processes to estimate the flow rate. The first one is the estimation of velocity profile in the pipe using the calculation described above. The second one is the calculation of time-series tracer diffusion using the new calculation domain, which focuses on only the inside pipe around sensor and ejection. The velocity profile estimated by first step is applied to that calculation domain and assumed to be stable. Then, comparison of time-series tracer concentration between numerical results and experimental one, which was obtained in 2004 [2], is conducted. Re-examination of steady velocity profiles is conducted if disagreement is observed.

Numerical Results
Flow Rate Estimation in Mariana Area

The calculation results of axial velocity profiles at several typical horizontal levels are shown in Figure 4. The velocity profiles are observed as M-shape flow except for distribution at the inlet of the pipe. This is because heat transfer from outside fluid does not reach to the pipe axis. The flow rate in Figure 4 is 166.8t/day. Figure 4 also shows that the reverse flow may occur near the axis at middle of the pipe. In the experiments, upwelling flow was measured continuously at the sensor point, which lied 13m below the pipe outlet. However downward flow might be measured if the sensors were laid at different point. Therefore axial velocity at the axis is investigated to confirm reverse flow area and shown in Figure 5. The reverse flow between 20m and 190m below the pipe outlet is shown.

Then, flow rate estimation is conducted using the method described above. The velocity profile of sensor point shown in Figure 4 is used. As a result, the comparison of time-series tracer concentration between numerical and experimental result is done and disagreement between the numerical simulation and the experimental one is obtained. The peak of time-series tracer concentration by numerical simulation is observed much earlier than that by experiment at two sensor points as shown in Figure 6. This indicated that the calculation results of velocity profiled shown in Figure 4 are over estimated.
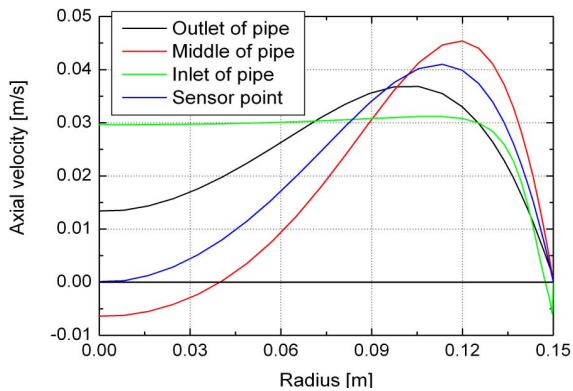
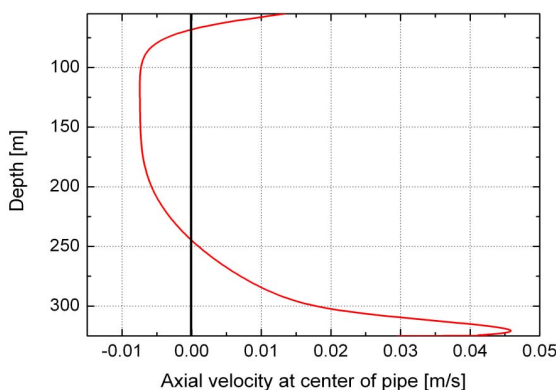Figure 4. Axial velocity profiles at several levels in the pipe

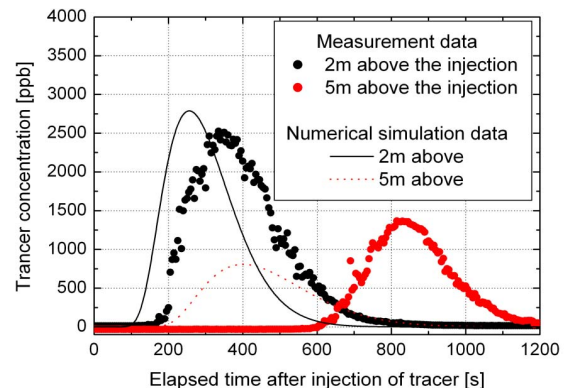Figure 5. Axial velocity distribution at the axis of the pipe

Figure 6. Comparison between measurement data and calculated data

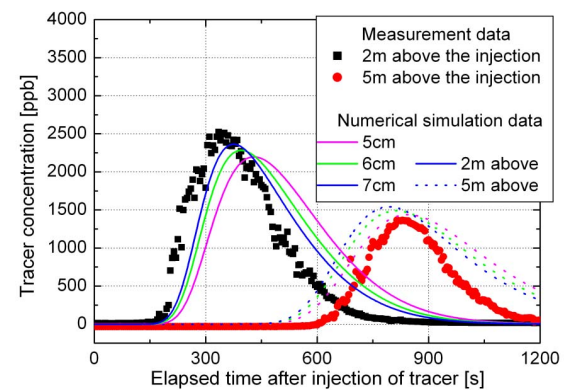Figure 7. Comparison between measurement data and corrected calculated data under the sensor inclined condition

Two factors are considered as the reason of over-estimation. The first factor is over-estimation of eddy diffusivity in the pipe. In this study, thermal conductivity and viscosity are estimated using the constant eddy diffusivity. However in reality, laminar sub layer exists and eddy diffusivity becomes less near the wall. Therefore this calculation may over estimates the heat transfer from outside the pipe. The second factor is inclination of the pipe. Three depth indicators were installed at top, middle and bottom of the pipe in experiment. In 2004 experiment, the measured value of depth at middle and bottom of the pipe was fluctuating even though the top of the pipe was almost stable [2]. This indicates that the pipe inclined. Therefore sensor location might be moved from the axis of the pipe and measurement point of the numerical simulation may not be same as that of experiment.

Accordingly for the overcome of first factor, eddy diffusivity is reconsidered. However it is difficult to provide distribution of eddy diffusivity, which includes wall effect, because there are no enough experimental data near the wall. Therefore velocity calculated above is reconsidered and velocity magnitude is modified to coincide with experimental data keeping M-shape flow. Furthermore for the overcome of second factor, the measurement points of tracer concentration are repositioned radially. Considering the depth indicator data and sensor length, the measurement point was predicted to move about 5cm far from the axis in 2004 experiment. Therefore new measurement points are positioned at 5cm, 6cm and 7cm far from the axis. As a result, it becomes clear that the time-series tracer concentration obtained by quarter of velocity profile calculated above is good agreement with experimental data at 7cm far from the axis as shown in Figure 7. This indicates that velocity profile in the experiment may be close to M-shape flow. Furthermore, the flow rate of 2004 experiment in Mariana area is predicted as 43t/day

by using modified velocity profile. This value is 4 times less than the case in Figure 4. This flow rate depends not only on temperature and salinity but also on wave conditions. Therefore it may decrease at same ocean area if the effect of pipe oscillation and deformation are small. Accordingly measurement diffusivity $10^{-5}m^2/s$ is assumed as maximum eddy diffusivity here.

Flow Rate Estimation in Other Ocean Area

As described above, there is an urgent need to create sea planting in pelagic zone because of problem with food product recently. Therefore not only Mariana area but also other pelagic areas should be paid attentions. However upwelling flow rate by perpetual salt fountain depends on ocean conditions and it is uncertain that enough flow rate can be obtained in all pelagic zone. Accordingly rough flow rate should be predicted in several pelagic zones before experiment. Therefore this section focuses on the possibility of flow rate estimation depending on ocean conditions numerically and discusses it with paying attention to 101.29E and 19.49S ocean area near Australia particularly.

The governing equations and calculation scheme are same as Mariana area case. The temperature and salinity distributions of the ocean area, which are obtained by GEOSECS (Geochemical Ocean Sections Study), are used as initial and boundary conditions. The pipe length is modified as 600m because the depth difference between maximum and minimum salinity is 600m. The depth of outlet pipe is same as that in Figure2. The assumptions are also same as previous one. In this calculation, molecular and measured diffusivity $10^{-5}m^2/s$ are used as minimum and maximum flow rate case. Several pipe diameters, 20cm, 30cm, 50cm, 100cm, are considered for the comparison.

The calculation result of flow rate at each condition is shown in Figure 8. The calculated flow rate increases with the increment of pipe diameter and increment rate of measured diffusivity is much larger than that of molecular diffusivity. This is the effect of boundary layer thickness. In the case of measured diffusivity, the effect of turbulent mixing is considered by the assumption that thermal diffusivity and kinematic viscosity are specified as measured diffusivity. Therefore viscosity and conductivity become much larger than molecular diffusivity case. As a result, thermal boundary layer thickness becomes much larger and flow rate increases dramatically when the diameter increases.

As described above, flow rate is affected by many factors. Therefore for the flow rate estimation at all ocean areas, unified representation of these factors should be done. Accordingly this study introduces new dimensionless number Ra_R, which was proposed by Takahashi et al [3]. The Ra_R is modification of Rayleigh number as shown in eq. (5).

$$Ra_R = \frac{gr^3}{\alpha v} \cdot \frac{R_\infty - R_i}{R_i}, \tag{5}$$

$$R_i = \int_0^L \rho_i dx, \tag{6}$$

$$R_\infty = \int_0^L \rho_\infty dx, \tag{7}$$

where g, α are gravity acceleration and thermal diffusivity. L, ρ_i, ρ_∞ are pipe length, inside and outside density. The Ra_R estimates the driving force of this calculation by the density difference between inside and outside pipe caused by temperature and salinity distributions.

The result of realignment with modified Ra_R is shown in Figure 9. The dimensionless flow rate shown in eq. (8) is used. Aihara et al. proposed this number in UWT (Uniform Wall Temperature) condition.

$$G = \frac{1}{\mu \cdot Gr \cdot r} Q, \tag{8}$$

where Q, μ, Gr are flow rate, viscosity and Grashof number. Figure 9 also includes the calculation results of Mariana area with molecular and measured diffusivity to evaluate the possibility of unified representation.

As a result, the relationship between dimensionless flow rate and modified Ra_R has same tendency even in different ocean conditions. This means that a unified representation of factors, which affect the flow rate, is achieved. As shown in Mariana experiment in 2004, the modification of flow rate is necessary in small Ra_R region, however Figure 8 shows that the possibility of flow rate estimation in all ocean conditions can be evaluated.

Conclusions

The numerical simulation for upwelling of deep seawater with the perpetual salt fountain is conducted in this study. As a result, the velocity profile of the upwelling experiment in Mariana area is predicted as M-shape flow and the possibility of reverse flow near the axis at middle of the pipe is indicated. Additionally flow rate is estimated as 43t/day in the pipe with some modifications. Furthermore the upwelling flow in 101.29E and 19.49S ocean area near Australia is calculated and flow rate estimation depending on ocean conditions is discussed. As a result, it becomes clear that the unified representation of ocean conditions is achieved by the introduction of new dimensionless number Ra_R, which is modified Rayleigh number, and the dimensionless flow rate can be evaluated by modified Ra_R.
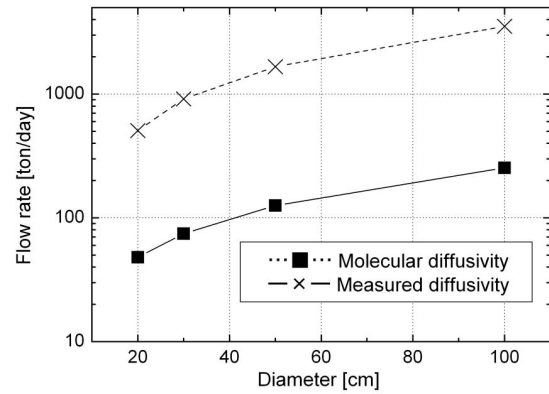

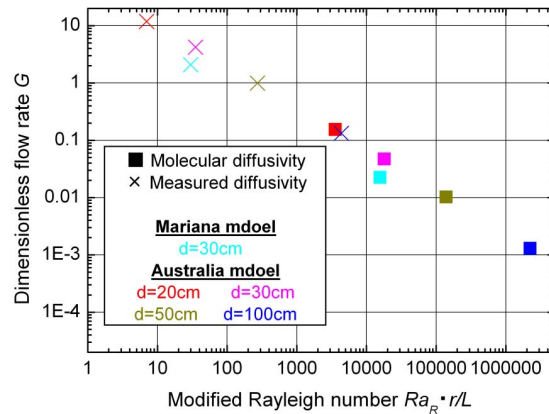Figure 8. Predicted flow rate in the ocean near Australia

Figure 9. Dimensionless flow rate at each condition

References

[1] H. Stommel, A.B. Arons & D. Blanchard, An oceanographical curiosity : the perpetual salt fountain, *Deep-Sea Res.*, **3**, 1956, 152-153.

[2] K. Tsubaki, S. Maruyama, A. Komiya, H. Mitsugashira, Continuous measurement of an artificial upwelling of deep seawater induced by the perpetual salt fountain, *Deep-Sea Res., Part I*, **54**, 2007, 75-84.

[3] N. Takahashi, S. Maruyama, S. Sakai, K & Taira, A numerical analysis of natural convection using temperature and concentration differences, *Report of the Institute of Fluid Science*, **13**, 2002, 21-30.

[4] P. Fofonoff, R. C. Millard Jr., Algorithms for computation of fundamental properties of seawater, *Unesco technical papers in marine science*, 1983.

[5] S. Maruyama, K. Tsubaki, K. Taira & S. Sakai, Artificial Upwelling of Deep Seawater Using the Perpetual Salt Fountain for Cultivation of Ocean Desert, *J. Oceanogr.*, **60**, 2004, 563-568.

[6] T. Dylan, Ocean thermal energy conversion: current overview and future outlook, *Renewable energy*, **6**, 1995, 367-373.

[7] T. Nakasone & S. Akeda, THE APPLICATION OF DEEP SEA WATER IN JAPAN, *UJNR Technical Report*, **28**, 1999, 69-75.

[8] X. R. Zhang, S. Maruyama, S. Sakai, K. Tsubaki & M. Behnia, Flow prediction in upwelling deep seawater − The Perpetual Salt Fountain, *Deep-Sea Res., Part I*, **51**, 9, 2004, 1145-1157.